Broadband Microwave Signal Processing Enabled by Polarization-Based Photonic Microwave Phase Shifters

Yamei Zhang, *Student Member, IEEE*, and Shilong Pan, *Senior Member, IEEE*

(Invited Paper)

***Abstract*— A polarization-based photonic microwave phase shifter that implemented with an orthogonal circularly-/linearly-polarized wavelength generator incorporated with a polarizer provides advantages of high scalability, high-speed phase tuning, large operation bandwidth, full-360-degree tunability, flat power response, and compact configuration, making it a key enabler for tunable microwave photonic filtering, optically controlled beamforming, high speed phase coding, large time-bandwidth product signal generation, phase noise measurement, and co-site RF signal cancellation. In this paper, the recent advances of polarization-based photonic microwave phase shifters are reviewed. A general model of the polarization-based photonic microwave phase shifter is established, and the applications of the polarization-based photonic microwave phase shifter are described and discussed.**

***Index Terms*— Microwave photonics, phase shifter, frequency multiplying, frequency mixing, signal processing.**

I. INTRODUCTION

SIGNAL processing for extraction, suppression, transformation, recognition, analysis, synthesis, and modification of an existing signal is widely used in radars, communications, and electronic warfare systems [1]–[3]. With the fast development of microwave, millimeter-wave and terahertz technologies, pre-processing of analog signals with high center frequencies and large instantaneous bandwidths in the analog domain would be more practical than the full-digital solution due to the lack of high performance and large bandwidth analog-to-digital converters (ADCs). Even if the high-performance ADCs can be achieved, the latency to deal with the huge amount of data after the ADCs would also be unbearable [4]. Although analog signal processing using purely electronic schemes are well developed [5], [6], they usually suffer from limited instantaneous bandwidth and complicated configurations. To overcome this problem, microwave photonic signal processing was proposed to pre-process the large-bandwidth signals in the optical domain, which provides distinct features in terms of high frequency, broad instantaneous bandwidth, low transmission loss and immunity to electromagnetic interference [7]–[10].

Microwave photonic signal processing is generally performed by upconverting the microwave signal to the optical domain and manipulating them with photonic approaches [9], [10]. Due to the factor that the frequency of the optical carrier is around 193 THz and that of the microwave signal is only tens of GHz, the fractional bandwidth of the optical microwave signal is very small, so it is quite easy for photonic systems to handle the broadband microwave signals. In the past decades, considerable efforts have been devoted to realizing various microwave photonic signal processing functions [7]–[10], of which the basis is how to manipulate the magnitude and phase of the microwave signals. Since the magnitude can be easily tuned by an optical attenuator or amplifier, a photonic microwave phase shifter is considered as a fundamental element and key technical enabler for many microwave photonic signal processing, such as tunable microwave photonic filtering, optically controlled beamforming, high-speed phase coding, large time-bandwidth product (TBWP) signal generation, high precision phase noise measurement, and RF interference cancellation. Therefore, the performance of these functions will be significantly influenced by the bandwidth, operational frequency range, tuning speed, and reconfigurability of the photonic microwave phase shifter.

Previously, different approaches were proposed to implement the photonic microwave phase shifter, which can generally be divided into three categories, i.e., slow-light-based method [11]–[15], optical vector-sum technique [16], [17], and optical heterodyne technique [18]–[22]. The slow-light-based photonic microwave phase shifter is implemented through slowing down the optical carrier and/or sidebands in a medium with a tremendous effective refractive index, so the phase of the signal can be continuously tuned by adjusting the time delay introduced by the slow light effect. The main problem associated with this method is the large power variation accompanied with the phase shifting thanks to the well-known Kramers-Kronig relations. The phase shifter based on the optical vector-sum technique is realized by combining two

Manuscript received April 18, 2018; revised June 2, 2018; accepted June 7, 2018. Date of publication June 14, 2018; date of current version June 28, 2018. This work was supported in part by the National Natural Science Foundation of China under Grant 61527820 and in part by the Fundamental Research Funds for the Central Universities. *(Corresponding author: Shilong Pan.)*

The authors are with the Key Laboratory of Radar Imaging and Microwave Photonics, Ministry of Education, Nanjing University of Aeronautics and Astronautics, Nanjing 210016, China (e-mail: pans@ieee.org).

Color versions of one or more of the figures in this paper are available online at http://ieeexplore.ieee.org.

Digital Object Identifier 10.1109/JQE.2018.2847398

TABLE I
COMPARISON OF THE TYPICAL PHOTONIC MICROWAVE PHASE SHIFTERS

Category	Ref.	Bandwidth	Phase shifting range	Power variations
Slow light method	[11]	14 GHz (1-15GHz)	0-240°	3 dB
	[12]	<1 GHz	0-360°	>40 dB
	[13]	Up to 40 GHz	0-360°	>10 dB
	[14]	8 GHz (24-32 GHz)	0-280°	Not mentioned
	[15]	Single frequency (40 GHz)	0-600°	2 dB
Vector-sum method	[16]	10 GHz (35-45GHz)	0-360°	4 dB
	[17]	8 GHz (8-16GHz)	<450°	18 dB
Polarization-based method	[23]	>30 GHz (10-40 GHz)	0-360°	<1 dB

microwave signals with different ratio of the initial phases in the optical domain. By adjusting the amplitude of the two signals, the phase of the combined signal can be tuned. Also, this method would suffer from severe power variation, and the configuration is usually complex [16], [17]. In the optical heterodyne technique, a phase difference is introduced to two phase-correlated wavelengths. Beating the two phase-correlated lightwaves at a photodetector (PD), a microwave signal is obtained, with its phase equaling to the phase difference of the two wavelengths. This method is simple, and the phase can possibly be tuned with no change of the amplitude [23].

The key challenge of the optical heterodyne technique is to introduce a phase difference to the two phase-correlated wavelengths while maintaining the phase correlations of them. To do so, polarization-sensitive modulators can be applied [23]–[38], which generate two orthogonal linearly- or circularly-polarized wavelengths. With a polarizer to combine the two wavelengths, a microwave signal with the phase continuously tuned by the polarization direction of the polarizer would be generated at a PD. Since the two wavelengths experience the same environmental variations in all the optical components, the phase correlations between the two wavelengths are maintained. The polarization-based photonic microwave phase shifters have the features of wide bandwidth, high tuning speed, flat power response and excellent scalability. Table I compares the performance of the typical microwave phase shifters in different categories.

In this paper, techniques for implementing the polarization-based photonic microwave phase shifters are discussed, and analog signal processing based on these phase shifters is overviewed and discussed with an emphasis on the operational principles and system architectures. The paper is organized as follows. In Section II, the principle of the polarization-based photonic microwave phase shifter is introduced, and techniques to generate two orthogonally-polarized wavelengths for the phase shifter are overviewed. In Section III, analog signal processing functions enabled by a polarization-based photonic microwave phase shifter are described, including microwave photonic filtering, optically controlled beamforming, high-speed phase coding, LFM signal generation, high-precision phase noise measurement, and RF interference cancellation. In Section IV, some concluding remarks and discussion are provided.

II. POLARIZATION-BASED PHOTONIC MICROWAVE PHASE SHIFTER

A. General Principle

To implement the polarization-based photonic microwave phase shifter, two circularly-polarized wavelengths with opposite rotation directions (which is also defined as orthogonal circularly-polarized wavelengths) should be generated first, which can be expressed as

$$E(t) = A_1 \exp(j\omega_1 t)\left[\exp\left(j\frac{\pi}{2}\right)\hat{x} + \hat{y}\right] + A_2 \exp(j\omega_2 t + j\phi_0)\left[-\exp\left(j\frac{\pi}{2}\right)\hat{x} + \hat{y}\right] \quad (1)$$

where x and y represent the two orthogonal polarization directions, ω_1 and ω_2 are the angular frequencies of the two wavelengths, A_1 and A_2 are the amplitudes, and φ_0 is a static phase difference between the two wavelengths. With a polarizer to combine the signals along the two polarization directions, the signal in (1) becomes,

$$\begin{aligned} E(t) &= A_1 \exp(j\omega_1 t)[j\sin\alpha + \cos\alpha] \\ &\quad + A_2 \exp(j\omega_2 t + j\phi_0)[-j\sin\alpha + \cos\alpha] \\ &= A_1 \exp(j\omega_1 t + j\alpha) + A_2 \exp(j\omega_2 t + j\phi_0 - j\alpha) \end{aligned} \quad (2)$$

where α is the angle between the polarization direction of the polarizer and one of the principal axes of the signal in (1). Directing the signal in (2) to a PD, the AC term of the output current is,

$$I_{AC}(t) \propto \frac{\Re A_1 A_2}{2}\cos[(\omega_1 - \omega_2)t + 2\alpha - \phi_0] \quad (3)$$

where $\Re$ is the responsivity of the PD. As can be seen from (3), a microwave signal is generated with a frequency that equals to the wavelength difference of the two wavelengths and a phase which is linearly proportional to the polarization angle α of the polarizer. By adjusting α, the phase of the microwave signal can be continuously tuned while the amplitude maintains unchanged. As a result, a photonic-assisted microwave phase shifter is implemented. Although (1)-(3) is obtained by single-microwave-frequency excitation, they are also suitable

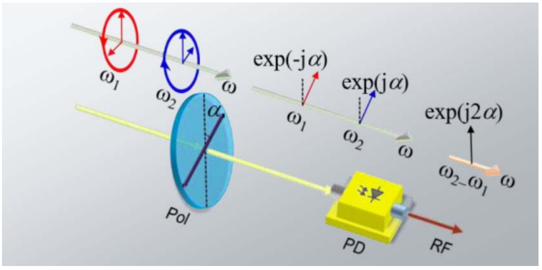

Fig. 1. The illustration of the polarization-based photonic microwave phase shifter. Pol: polarizer; PD: photodetector.

for broadband excitation, by which $A_2 \exp(j\omega_2 t + j\phi_0)$ in (1) is replaced by $\sum_{n=2}^{\propto} A_n \exp(j\omega_n t + j\phi_n)$ if small-signal modulation is assumed.

Since the phase shift is solely adjusted by the polarizer, the system can be easily scaled to implement independent multi-channel phase shifting, by splitting the two circularly polarized wavelengths into a number of channels and each channel incorporates with a polarizer. In addition, the phase shifter can be tuned with an ultra-high speed if the polarizer is replaced by an electrically-controlled polarizer.

B. Generation of Orthogonal Linearly-Polarized Wavelengths

From (1)-(3), the generation of two orthogonal circularly-polarized wavelengths is the key to implement the polarization-based photonic microwave phase shifter. To obtain the two circularly-polarized wavelengths, one can first generate two orthogonal linearly-polarized wavelengths, and then converting the two wavelengths from linear polarization to circular polarization via a polarization controller (PC). Mathematically, the two linearly-polarized wavelengths can be represented as,

$$E(t) = A_1 \exp(j\omega_1 t)\,\hat{x} + A_2 \exp(j\omega_2 t + j\phi_0)\,\hat{y} \tag{4}$$

If a PC is used to rotate the two wavelengths in (4) by 45 degree (denote the new orthogonal polarization directions as x' and y') and introduce an additional phase shift of 90 degree between x' and y', the signal in (4) can be rewritten as

$$\begin{aligned} E(t) \propto\ & \left[A_1 \exp(j\omega_1 t) - A_2 \exp(j\omega_2 t + j\phi_0)\right] \exp\left(j\frac{\pi}{2}\right)\hat{x}' \\ & + \left[A_1 \exp(j\omega_1 t) + A_2 \exp(j\omega_2 t + j\phi_0)\right]\hat{y}' \\ =\ & A_1 \exp(j\omega_1 t)\left[\exp\left(j\frac{\pi}{2}\right)\hat{x}' + \hat{y}'\right] \\ & + A_2 \exp(j\omega_2 t + j\phi_0)\left[-\exp\left(j\frac{\pi}{2}\right)\hat{x}' + \hat{y}'\right] \end{aligned} \tag{5}$$

As can be seen, a signal which has the same expression of (1) is obtained. Therefore, if the two orthogonal linearly-polarized wavelengths can be generated, the polarization-based photonic microwave phase shifter can be easily realized.

An intuitional way to generate the two orthogonal linearly-polarized wavelengths is to combine two phase-correlated optical wavelengths with a polarization beam combiner (PBC) [24]–[26]. One critical problem associated with this method is that the two wavelengths must be spatially separated before the PBC, as shown in Fig. 2 (a), which would introduce serious phase jitter to the generated microwave signal.

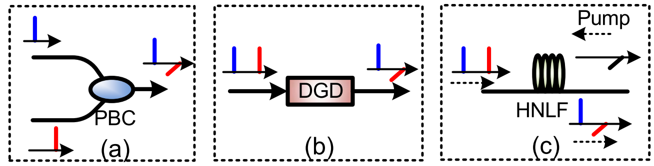

Fig. 2. The illustration of the (a) PBC-, (b) DGD- and (c) SBS-based orthogonally-polarized wavelength generator. HNLF: highly nonlinear fiber.

Another method for the generation of the orthogonal linearly-polarized wavelengths is based on first-order polarization mode dispersion (PMD) [27]–[29]. The principle of this kind of approach is illustrated in Fig. 2 (b). When two phase-correlated wavelengths are applied to a differential group delay (DGD) element with a DGD value of τ, the polarization states of them would be rotated by different polarization angles. The angle difference is $\Delta\omega\tau$, where $\Delta\omega = \omega_2 - \omega_1$ represents the angular frequency of the microwave signal. If the DGD is selected to let $\Delta\omega\tau = (2n+1)\pi/2 (n = 1, 2, 3\ldots)$, the two wavelengths are orthogonally polarized. In [28], a polarization-maintaining fiber (PMF) is utilized as the DGD element, and in [29], a specially-designed polarization-maintaining FBG (PM-FBG), which has two spectrally separated and orthogonally polarized transmission bands is used to make the two wavelengths orthogonally polarized. The key problem of the PMD-based method is that the DGD-induced polarization rotation is frequency dependent, so only the wavelengths separated by several specific frequencies can be made orthogonal.

The orthogonal linearly-polarized wavelengths can also be generated by stimulated Brillouin scattering (SBS) based polarization rotation. When an optical signal is amplified by the SBS gain in the fiber, the state of the polarization (SOP) of the amplified signal will be evolved towards the SOP of the pump signal [39], as shown in Fig. 2 (c). Therefore, if a pump signal with an orthogonal polarization state is applied to amplify an optical signal [30], the SOP of the signal after amplification could be orthogonal to the original one. However, cross-polarization SBS gain is usually very small. To ensure a sufficiently large polarization rotation when the pump signal is orthogonal with the signal to be amplified, large pump power [30] or several stages of SBS must be employed [31], leading to high power consumption or a complicated structure.

C. Direct Generation of Orthogonal Circularly-Polarized Wavelengths

The two orthogonal circularly-polarized wavelengths for realizing the polarization-based photonic microwave phase shifter can also be directly generated based on polarization modulation [23], [32]–[37].

Different from the conventional electro-optical intensity modulation and phase modulation, polarization modulation operates on the polarization state of a lightwave, which can be performed by cross-polarization modulation in an SOA [40], nonlinear polarization rotation in highly nonlinear

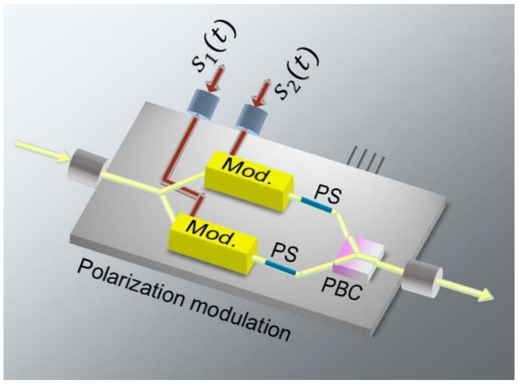

Fig. 3. The general scheme for implementation of polarization modulation.

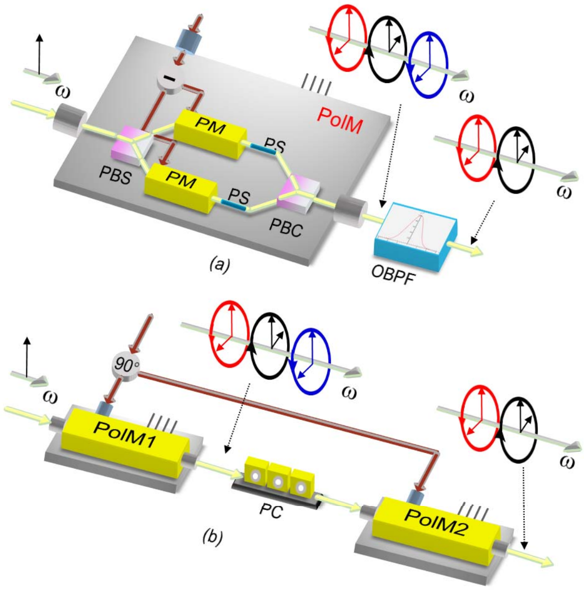

Fig. 4. Schemes for generating orthogonal circularly-polarized wavelengths: (a) based on a PolM and an OBPF; (b) based on two cascaded PolMs.

mediums [41], a phase modulator (PM) without an input polarizer [42], a GaAs-based polarization modulator (PolM) [43], or a polarization division multiplexing (PDM) Mach-Zehnder modulator (MZM) [44]. Fig. 3 shows the general model of the methods to implement the polarization modulation, in which, different modulations are introduced to the TE and TM modes of an input lightwave. For the GaAs-based PolM and the PM without an input polarizer, the modulations are phase modulations with different modulation indices, while for PDM-MZMs the modulations are intensity modulations.

In [23], a GaAs-based PolM incorporated with an optical bandpass filter (OBPF) was employed to generate the two orthogonal circularly-polarized wavelengths, as shown in Fig. 4 (a). When a lightwave is injected into the PolM, two complementary phase-modulated signals are generated along the two orthogonal polarization directions. One phase-modulated signal consists of two 1^{st}-order sidebands with a phase of $\pi/2$ and an optical carrier with a phase of 0, while the two 1^{st}-order sidebands in the other phase-modulated signal have a phase of $-\pi/2$. Introducing an additional phase difference of $\pi/2$ to the signals by a DC bias to the PolM, the phase difference between the orthogonally-polarized components are $\pi/2$ for the $\pm1^{st}$-order sidebands and $-\pi/2$ for the optical carrier, respectively. Therefore, the output of the PolM comprises three circularly-polarized wavelengths, among which the $\pm1^{st}$-order sidebands have the same rotation directions while that the optical carrier rotates in the opposite direction. With an OBPF to remove one of the $\pm1^{st}$-order sidebands, two circularly polarized wavelengths with opposite rotation directions are left. Based on this signal, a photonic microwave phase shifter with an operational frequency range from 10 to 40 GHz and a very small power variation (<1 dB) was realized [23]. The major problem with this method is that the OBPF always has a relatively small slope, which limits the lowest operational RF frequency to 10 GHz.

Another method to generate the two orthogonal circularly-polarized wavelengths is based on two cascaded PolMs [32], as shown in Fig. 4 (b). Three circularly-polarized sidebands are first generated at the output of the first PolM (PolM1) which is driven by an RF signal. Different from the direct filtering method in [23], a second PolM (PolM2) is followed to modulate the three circularly polarized sidebands with a quadrature RF signal. After PolM2, one of the newly generated $\pm1^{st}$-order sidebands of the optical carrier will be phase canceled with the original one while the other sideband is enhanced. As a result, only two wavelengths remain. The phase difference between the two orthogonally-polarized components of the two remained wavelengths are $\pi/2$ and $-\pi/2$, respectively, indicating that two orthogonal circularly-polarized wavelengths are generated. In an experiment, the undesirable first-order sideband was suppressed by 30 dB as compared to the remaining one, and the system can be operated in the frequency range of 2 to 36 GHz, which is limited by the bandwidth of the electrical 90-degree hybrid. Compared with [23], the lower frequency boundary is significantly decreased.

D. Generation of Orthogonally-Polarized Wavelengths With Multiplied Frequency Spacing

For the above methods, the maximum operating frequency is limited by the bandwidth of the electro-optical modulators and the electrical devices used in the system. To break the bandwidth limitation, approaches that can perform simultaneously frequency multiplication and phase shifting are highly desirable [28], [29], [33]–[35]. The key is to generate two orthogonally-polarized wavelengths separated by a frequency that is multiple times of the frequency of the input RF signal.

Previously, a DGD element, e.g., a PMF [28] or a PM-FBG [29], was employed to generate the orthogonally polarized $\pm1^{st}$-order sidebands or $\pm2^{nd}$-order sidebands. Again, the DGD-induced polarization rotation is frequency dependent, so the method is effective at several frequencies only.

To solve this problem, a dual-parallel PolM (DP-PolM) was used to generate the circularly-polarized $\pm1^{st}$-order sidebands [33]. The equivalent structure of the DP-PolM is illustrated in Fig. 5 (a), which comprises of two sub-PolMs,

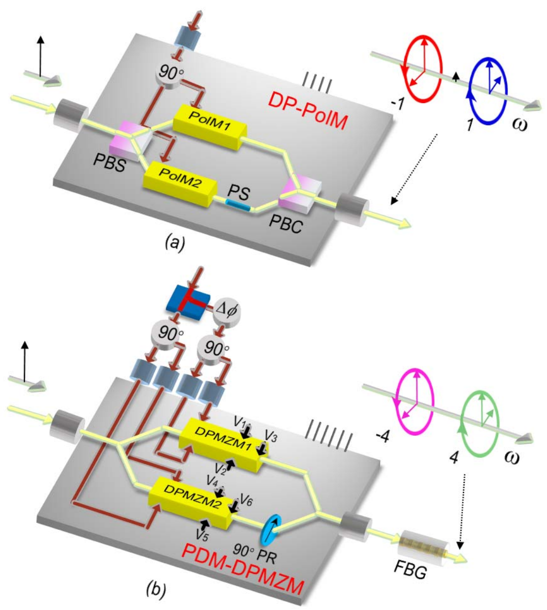

Fig. 5. Schemes for the generation of orthogonal circularly-polarized wavelengths with multiplied frequency spacing: (a) based on a DP-PolM; (b) based on a PDM-DPMZM.

a polarization beam splitter (PBS), and a PBC. Since each input port of the PBC only adopts lightwaves with specific polarization states, it serves as a polarizer for the output signal from each sub-PolM of the DP-PolM. According to [45], a PolM followed by a polarizer would perform as an MZM. The upper equivalent MZM is driven by an RF signal, which generates two first-order sidebands with an identical phase along one polarization direction. Meanwhile, the lower MZM is driven by a quadrature RF signal, so the $\pm1^{st}$-order sideband would have a phase of $\pm\pi/2$, respectively, along the orthogonal polarization direction. Both MZMs are biased at the minimum transmission point (MITP), which performs carrier suppression. Two orthogonal circularly-polarized sidebands are therefore generated, as the phase difference between the two -1^{st}-order sidebands along the two orthogonal polarization directions is $\pi/2$ while that of the $+1^{st}$-order sidebands is $-\pi/2$. If the two wavelengths are sent to a PD, a microwave signal with a frequency that is two times of the frequency of the input RF signal will be generated. The frequency doubling operation makes the system work at a frequency range beyond the bandwidth of the electrical devices.

To further increase the frequency range, orthogonal circularly-polarized $\pm1^{st}$-order sidebands, $\pm2^{nd}$-order sidebands and $\pm4^{th}$-order sidebands were generated by using a PDM dual-parallel MZM (PDM-DPMZM) [36], [37], as shown in Fig. 5 (b), which can be applied for the generation of microwave signals with frequency multiplication factors (FMFs) of 2, 4, and 8. The PDM-DPMZM is driven by four RF signals. To obtain the four RF signals, the output of a RF source is first split into two paths with an electrical divider, which also introduce a fixed phase shift $\Delta\varphi$ to one path [36]. Then, the two RF signals are further split into four paths with two electrical 90-degree hybrids. Table II shows the values of $\Delta\varphi$ and the phase shifts introduced by the DC biases for achieving different FMFs. When the phase shift $\Delta\varphi$ is controlled to be 0, $\pi/4$ or $\pi/8$, and the DC biases are properly set, two orthogonal circularly-polarized wavelengths that separated by 2, 4 or 8 times of the frequency of the electrical driven signals are generated, respectively. The evolutions of the optical spectra at different positions in Fig. 5(b) for different FMFs are illustrated in Fig. 6.

TABLE II
THE PHASE SET OF RF SIGNAL AND THE PHASE SHIFTS INTRODUCED BY THE DC BIASES FOR DIFFERENT FMFS

FMF	$\Delta\phi$	φ_{DCi} (i=1,2…6)
2	0	π,π,0,π,π,π
4	π/4	0,0,π,0,0,π
8	π/8	0,0,0,0,0,0

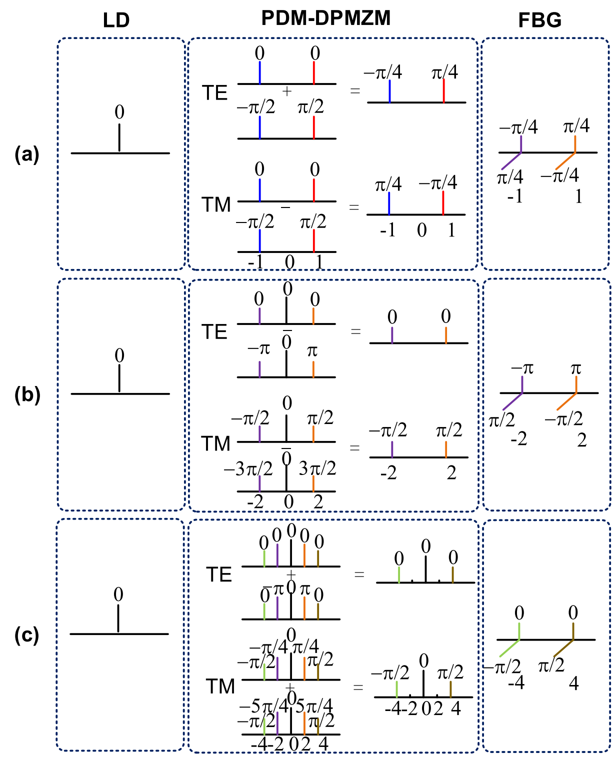

Fig. 6. The illustrations of the optical spectra at different positions for FMFs of (a) 2, (b) 4, and (c) 8.

The PDM-DPMZM can also be applied to perform phase shifting with frequency conversion [38]. The two sub-DPMZMs of the PDM-DPMZM are driven by two pairs of quadrature RF signals with different frequencies, which are obtained by splitting the outputs of two RF sources via two 90-degree hybrids, respectively, as shown in Fig. 7. By adjusting the DC biases of the PDM-DPMZM, a carrier-suppressed single sideband (CS-SSB) modulated signal with $+1^{st}$- or -1^{st}-order sideband suppressed can be generated by each sub-DPMZM. If one of the sub-DPMZMs generates a CS-SSB modulated signal with the $+1^{st}$-order sideband while the other sub-DPMZM produces a CS-SSB modulated signal with the -1^{st}-order sideband, two orthogonally-polarized wavelengths that separated by the sum

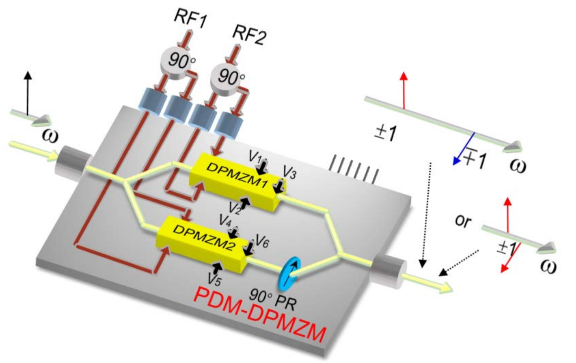

Fig. 7. Generation of two orthogonally polarized wavelengths that separated by the sum or the difference frequency between the two driven signals.

frequency of the two input RF signals can be generated at the output of the PDM-DPMZM. On the other hand, if the two sub-DPMZMs generate two CS-SSB modulated signals with the same sideband, two orthogonally-polarized wavelengths that separated by the difference frequency of the two input RF signals can be generated. In [38], a photonic microwave phase shifter with frequency conversion capability was built based on the PDM-DPMZM. With one of the frequencies of the RF signals fixed at 10 GHz, a frequency down-converted phase shifter over 0 to 13 GHz and a frequency up-converted phase shifter over 10 to 33 GHz were realized, and both phase shifters can be continuously tuned over 360 degree.

It should be noted that although the SOP of a light is very sensitive to the environment, the polarization-based photonic microwave phase shifter can still maintain stable because it is always operated locally which can be well packaged. In addition, adaptive polarization control might be applied for further stability improvement.

III. Applications of the Polarization-Based Photonic Microwave Phase Shifter

In this section, the recent advances of analog signal processing functions enabled by polarization-based photonic microwave phase shifter are reviewed and discussed, including finite impulse response (FIR) microwave photonic filtering, optical RF beamforming, phase-coded or linear frequency modulated (LFM) signal generation, high-precision phase noise measurement, and RF interference cancellation.

A. Tunable FIR Microwave Photonic Filter (MPF)

FIR MPF is one of the fundamental elements for microwave photonic signal processing, which can be realized by summing up N time-delayed and tap-weighted photonic microwave signals [7]–[10], [46], [47]. The electrical transfer function of an N-tap MPF is given by,

$$H(f) = \sum_{n=0}^{N-1} a_n \exp(-j2\pi f n T_{\mathrm{F}}) \tag{6}$$

where a_n $(n = 1, 2, \ldots, N)$ is the tap coefficients, f is the frequency of the filtered microwave signal, and T_{F} is the unit delay between the adjacent taps of the MPF. According to the coefficients, MPFs can be divided into three categories, i.e., positive-coefficient MPFs for low-pass filtering [48], [49], negative-coefficient MPFs for bandpass filtering [50]–[52], and complex-coefficient MPFs [53]–[64]. Among them, the frequency response of the complex-coefficient MPFs can be tuned without affecting the shape of the frequency response, which is highly desired for practical applications. The transfer function of a complex-coefficient MPF can be expressed as,

$$\begin{aligned} H'(f) &= a_0 + a_1 \exp(j\theta)\exp(-j2\pi f T_{\mathrm{F}}) \\ &\quad + a_2 \exp(j2\theta)\exp(-j2\pi f 2T_{\mathrm{F}}) \\ &\quad + \cdots + a_n \exp(jn\theta)\exp(-j2\pi f n T_{\mathrm{F}}) \\ &= \sum_{n=0}^{N-1} a_n \exp\left[jn2\pi T_{\mathrm{F}}\left(\frac{\theta}{2\pi T_{\mathrm{F}}} - f\right)\right] \end{aligned} \tag{7}$$

where θ is the phase difference between the adjacent taps (suppose the phase shift of the first tap is 0). From (7) we can see that the center frequency of the filter is $\theta/2\pi T_{\mathrm{F}}$. By adjusting the phase difference, the center frequency can be continuously tuned while the magnitude of the MPF maintains unchanged.

Therefore, the key to implement an MPF with complex coefficients is to realize one or more photonic microwave phase-shifted taps. Almost all the photonic microwave phase shifters can be employed to realize a complex coefficient in an MPF. Previously, the complex coefficient was implemented using SBS-based [53], [54], SOA-based [55], FBG-based [56], or external-modulated [57]–[63] photonic microwave phase shifters. However, most of these systems can realize only one complex coefficient. In addition, the modulus of the complex coefficients would be varied due to the phase-magnitude dependence of the phase shifter. To deal with the problems, a polarization-based photonic microwave phase shifter can be employed. Since the phase shift of the polarization-based photonic microwave phase shifter is solely adjusted by a polarizer followed by the orthogonal circularly-polarized wavelength generator, it can be easily scaled to implement multiple independent complex coefficients by splitting the output of the orthogonal circularly-polarized wavelength generator into N paths and each path incorporated with a polarizer. Thanks to the power-invariable phase shifting of the polarization-based photonic microwave phase shifter, the phase of the implemented complex coefficient can be continuously tuned while the modulus of the complex coefficients maintains unchanged. Summing up the N phase-shifted taps by a coupler or a wavelength-division multiplexer (WDM), an N-tap MPF can be realized. In [63], a 4-tap full-complex-coefficient MPF was realized by using a photonic microwave phase shifter based on a PolM and an OBPF. The frequency response of the 4-tap MPF can be continuously tuned over the full free spectral range (FSR) by adjusting the phase shifts of each tap.

Most of the previously reported MPFs with complex coefficients can only realize fundamental frequency signal filtering. In practice, however, simultaneous frequency mixing and tunable filtering are highly desired for most RF frontends. The frequency-mixed MPF can possibly be realized based on a frequency-mixed photonic microwave phase shifter [65], [66]. However, the phase shifters in [65] and [66] are tuned by

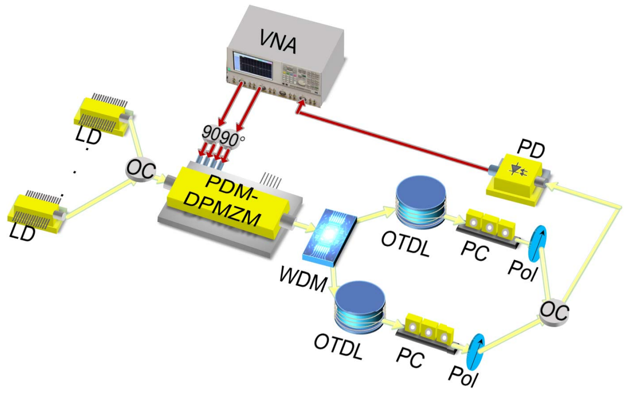

Fig. 8. The schematic diagram of the frequency mixed MPF. LD: laser diode; OC: optical combiner; OTDL: optical tunable delay line; WDM: wavelength division multiplexer; PC: polarization controller; Pol: polarizer; VNA: vector network analyzer.

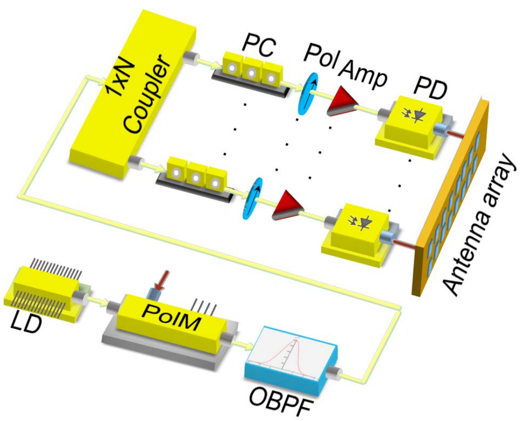

Fig. 9. The schematic diagram of the proposed OBFN. OBPF: optical bandpass filter; PBS: polarization beam splitter; PD: photodetector.

the DC biases of the electro-optic modulators, which requires multiple modulators to form multiple adjustable taps. To deal with this problem, a 4-tap frequency-mixed MPF was built based on the afore-mentioned polarization-based frequency-mixed phase shifter [38], as shown in Fig. 8. Each tap of the MPF realizes a frequency-mixed phase shifting, which can be continuously tuned over −180 degree to 180 degree by adjusting the PC in each tap. Therefore, the center frequency of the MPF can be continuously tuned over the full FSR while the shape of the frequency response maintains unchanged. The MPF can be switched between frequency up-conversion and down-conversion modes by adjusting the DC biases of the PDM-DPMZM. Frequency up-converted and down-converted MPFs were proved to be effective over 10-33 GHz and 0-13 GHz, respectively, when an RF signal fixed at 10 GHz was applied.

B. Optically Controlled Beamforming Network (OBFN)

Beamforming plays a significant role in modern radars and wireless communications [1], where high directionally transmitting or receiving of signals are required. The main principle of beamforming is to control the time delay or the phase of each radiated signal in a phased array antenna so that all the radiated signals have the same phase in the desired direction. Thanks to the inherent advantages offered by the photonic technology, such as small size, broad bandwidth, low transmission loss, large tunability, and immunity to electromagnetic interference, it is of great interests to implement the beamforming network in the optical domain [2], [3], [7]–10].

Previously, a lot of methods have been reported to realize the OBFN [67]–[72], which can mainly be divided into two categories. One is based on true time delay units [67]–[69], and the other is using photonic microwave phase shifters [70]–[72]. Although the true-time-delay based OBFN can realize squint-free beamforming over a broad bandwidth [67]–[69], OBFNs based on photonic microwave phase shifters are still interesting if the instantaneous bandwidth is not large. Since the photonic microwave phase shifters can operate over a broad frequency range, the photonic microwave phase shifter based OBFNs can be used in a frequency-agile system to realize phased array antennas with different center frequencies.

A typical photonic microwave phase shifter based OBFN was reported by Yi *et al.* [72], in which a programmable photonic processor based photonic microwave phase shifter was employed. The method is flexible since the photonic processor can manipulate the amplitude and phase of different optical spectral components independently. A 4-channel phase shifted OBFN was realized. However, the state-of-the-art photonic processor is still complicated, lossy and costly, and the scalability is limited by the number of the output ports of the photonic processor (typically $\leq$16).

Due to the excellent scalability of the polarization-based photonic microwave phase shifter, multi-channel phase shifting can be easily obtained; an OBFN can thus be realized. In [73], a polarization-modulated photonic microwave phase shifter based on a PolM and an OBPF is employed to realize an OBFN, as shown in Fig. 9. The PolM cascaded with the OBPF generates two circularly-polarized and oppositely-rotated wavelengths [23], which are then split into N paths, and each path is followed by a PC, a polarizer, and a PD to realize N phase shifters. By adjusting the PC in each path, the phase of the signal at the output of each PD can be continuously tuned [23], so the far-field radiation pattern can be changed. The phase shifter has a wide operation bandwidth (10-40 GHz in [23]) and flat power response, so the proposed OBFN is suitable for frequency-agile phased array antennas. In addition, the PolM-based circularly polarized and oppositely-rotated wavelength generator can be replaced by the PDM-DPMZM based generator so that frequency-mixed or frequency-multiplied OBFNs can also be realized.

C. Phase-Coded / LFM Signal Generation

Generation of microwave phase-coded signals or LFM signals has been widely investigated in the past decades for pulse compression in radar systems [1]. Thanks to the high frequency and large operational bandwidth provided by the photonic technologies, various schemes were proposed to generate phase-coded and LFM signals in the optical domain [33], [35], [36], [74]–[82].

Generally, a phase-coded signal or an LFM signal can be expressed as,

$$E_{\mathrm{p}}(t) = A_{\mathrm{p}} \cos\left[\omega_{\mathrm{p}} t + s\left(t\right)\right] \tag{8}$$

where A_{p}, ω_{p} and $s(t)$ are the amplitude, angular frequency and phase term of the phase-coded or LFM signal, respectively. When $s(t)$ is a sequence of electrical coding signal, $E_{\mathrm{p}}(t)$ stands for a phase-coded signal [80]. When $s(t)$ is a parabolic signal, $E_{\mathrm{p}}(t)$ represents an LFM signal [81], [82]. Therefore, the key to generating such a signal is to manipulate the phase of an RF signal according to $s(t)$, which is exactly what a photonic microwave phase shifter adept at. However, some of the photonic microwave phase shifters can be only effective for the generation of a very low-speed phase-coded signal due to the relatively slow phase tuning speed (~kHz). And some of them are power variable during phase tuning, which would decrease the compression performance of the generated signal. Thanks to the power-invariable phase shifting capability and ultra-high phase tuning speed (as high as 40 Gb/s [43]) of the polarization-based photonic microwave phase shifters, a high-speed phase-coded signal or a large-bandwidth LFM signal can be generated when an electrical coding signal or a parabolic signal is applied to the polarization-based photonic microwave phase shifters. The center frequency can be the fundamental frequency [80], the multiplied frequency [33], [35], [36], or the mixed frequency of the electrical RF driven signals. The coding speed can be as high as 40 Gb/s [43], limited by the bandwidth of the electrically-controlled polarizer used in the polarization-based photonic microwave phase shifters.

One key parameter to evaluate the generated signal is the TBWP, which is defined as the product of the time duration and the bandwidth of the generated signal. For a phase-coded signal generated based on the polarization-based photonic microwave phase shifter, its bandwidth equals to the coding speed and its time duration is related to the sequence length of the driven electrical coding signal. When the coding speed is fixed, the TBWP can be easily improved by increasing the sequence length of the driven signal.

For an LFM signal generated based on the polarization-based photonic microwave phase shifter, its bandwidth is related to the derivation of the phase variations with respect to the time and its time duration equals to the time duration of the driven parabolic signal. When the time duration is fixed, the larger the phase variation introduced by the parabolic signal is, the larger the bandwidth and TBWP is. However, the total phase variation introduced by the parabolic signal is generally smaller than 10 rad which is limited by the maximum tolerable power of the electrically-controlled polarizer [81]. Therefore, to improve the TBWP of the generated LFM signal, one has to increase the total phase variations introduced by the parabolic signal. To do so, *Li and Yao* used a recirculating phase modulation loop (RPML) to introduce a parabolic phase modulation during each recirculation, so the accumulated phase variation and the TBWP of the generated LFM signal were increased by tens of times [81]. However, the circulation times are limited due to the insertion loss of the devices used in the loop.

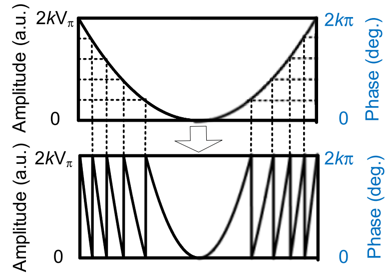

Fig. 10. Schematic of the conventional parabolic signal (upper) and the split parabolic signal (lower) when the split number equals to 10.

Another method to improve the TBWP of the LFM signal is using a spliced parabolic signal to drive the electrically-controlled polarizer. The spliced parabolic signal is obtained by splitting the conventional parabolic signal into N pieces, and each piece has the same amplitude, as shown in Fig. 10. By carefully designing the amplitude of the spliced parabolic signal to let the induced phase variation of each piece be 2π or the integral multiples of 2π, the total phase variations can be improved by $N/2$ times. Therefore, the TBWP of the generated signal can be improved by $N/2$ times too. An experiment in [82] demonstrated that an LFM signal with a TBWP of about 3846.2 was generated by using a 1000-piece parabolic signal. Compared to the case using an unsplit parabolic driven signal, the TBWP was improved by more than 500 times. It should be noted that the spliced parabolic phase modulation method can be applied in the aforementioned RPML [81] to generate even wider bandwidth LFM signals, so very large TBWPs (e.g., more than 10,000) might be possibly generated.

D. High Accuracy Phase Noise Measurement

Microwave signal with ultra-low phase noise is of particular importance in modern radar systems, wireless communications and measurement systems. With the assistance of photonic technologies, a 10-GHz microwave signal with ultra-low phase noise (-163 dBc/Hz@ 6 kHz) can be generated by an opto-electronic oscillator (OEO) [83]. However, it is challenging to measure such a low phase noise with the traditional phase noise measurement methods, including the direct spectrum method, the phase detector method [84]–[86], and the electrical-delay-line-based frequency discriminator method.

Compared with the other two methods, the delay-line-based frequency discriminator method is more likely to break out the sensitivity limitation, because the sensitivity of the frequency discriminator method is mainly determined by the amount of time delay introduced by the delay line, which can be significantly increased by optical delay line. Thanks to the high frequency, broad bandwidth, and ultra-low transmission loss brought by photonic technologies, the photonics-assisted phase noise measurement method based on optical delay line is supposed to be an effective way to reach an ultra-high sensitivity and a broad measurement bandwidth [87]–[91].

A high-sensitivity and large-bandwidth phase noise measurement system using optical delay line and polarization-based photonic microwave phase shifter was reported in [91],

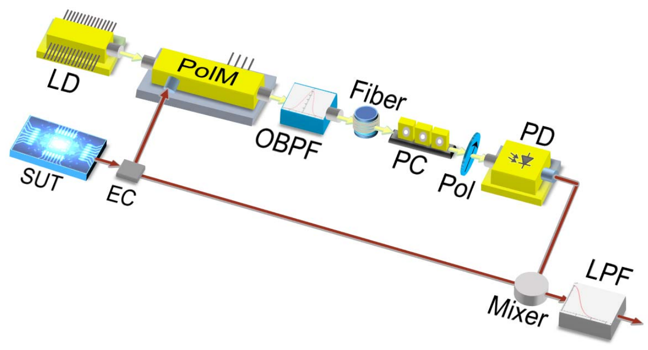

Fig. 11. The schematic diagram of the delay-line and photonic microwave phase shifter based phase noise measurement system. SUT: signal under test; LPF: low noise amplifier.

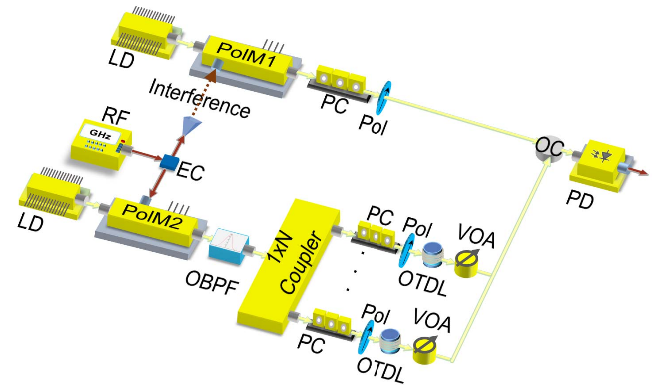

Fig. 12. The schematic diagram of the optical multipath RF interference cancellation system using a PolM-based photonic microwave phase shifter.

as shown in Fig. 11. The signal under test is first split into two replicas. One replica is time delayed by the optical delay line (e.g., a length of optical fiber) and phase shifted by the polarization-based photonic microwave phase shifter [23]. The delayed and phase-shifted replica is then mixed with the other replica of the microwave signal under test. Since the photonic microwave phase shifter can be continuously tuned from −180 to 180 degree [23], a quadrature phase difference between the two replicas which is necessary for the frequency discriminator can be easily satisfied. With an FFT analyzer, the phase noise can be easily calculated. A large measurement bandwidth in a range from 5 to 40 GHz and an ultra-low phase noise floor of −133 dBc/Hz@ 10 kHz was experimentally demonstrated.

It should be noted that, if frequency-multiplied photonic microwave phase shifters are employed in the system, the sensitivity of the phase noise measurement system may be improved [92].

E. Co-Site Interference Cancellation

With the fast development of the wireless communication and modern radar systems, the universally existed co-site interference would severely confine the performance of those systems. The co-site interference arises mainly from the electromagnetic interference between the transmitters and the receivers, i.e., the transmitted signals would interfere with the signal-of-interest (SOI) from a certain receiver. If the interference signal overlaps with the SOI, it cannot be removed with a filter. Therefore, co-site interference cancellation technologies must be employed.

To suppress the co-site interference, a cancellation signal that has the same amplitude and an opposite phase to the interference signal should be generated, which can be obtained by using a phase shifter and a variable attenuator. When the generated cancellation signal combines with the received signals, the interferences can be successfully removed [93]–[98]. Thanks to the broad bandwidth of photonic technology, a broadband optical RF interference cancellation system can be realized with a microwave photonic phase shifter. A typical optical RF interference cancellation system consists of two optical links, one of which is used to carry the SOI and the interference signal received from the antenna, and the other is employed to generate and transmit the cancellation signal by using a microwave photonic phase shifter and a variable optical attenuator (VOA). In [99], an RF interference cancellation system was built incorporating a DPMZM-based microwave photonic phase shifter. By adjusting the bias voltages of the DPMZM, the phase of the cancellation signal can be continuously tuned. Cooperated with a VOA, the co-site interference signal can be suppressed at the output of the PD.

However, the structure above did not take into account the conditions that the interference signal might be reflected, scattered or diffracted by the surroundings in a realistic scenario. So the received signals may contain multiple delayed, attenuated and phase-shifted copies of the interference signal. Therefore, a multipath cancellation structure must be employed to cancel each copy of the interference signal. However, the structure in [99] is difficult to be scaled without multiple DPMZMs, which would significantly increase the cost and complexity of the system. Since the polarization-based microwave photonic phase shifters have good scalability, they can be easily scaled to realize multi-path phase shifting with independent control of the phase. A multi-path interference cancellation structure has been proposed utilizing a PolM-based microwave photonic phase shifter [100], as shown in Fig.12. A 20-dB suppression over 13 GHz (from 3.5 GHz to 16.8 GHz) and a 30-dB suppression across 10 GHz (from 5.5 GHz to 15 GHz) were demonstrated.

IV. Conclusion and Discussion

In conclusion, the recent advances in polarization-based photonic microwave phase shifters were reviewed. The general principle and the system architectures with or without frequency-multiplication and frequency-conversion capability were introduced. Analog signal processing functions enabled by the polarization-based photonic microwave phase shifters (e.g., tunable FIR microwave photonic filtering, optical RF beamforming, phase-coded or LFM signal generation, high-precision phase noise measurement and RF interference cancellation) were described.

In addition to the signal processing functions mentioned in this paper, a polarization-based photonic microwave phase shifter may have the potential to realize an image-reject mixer [65] and a Hilbert transformer [101], since the intrinsic of these functions is to manipulate the phases of the input signals.

Meanwhile, the multi-functional signal processor can also be realized based on the polarization-based photonic microwave phase shifter. Thanks to the excellent scalability of the polarization-based photonic microwave phase shifter, multiple channels of phase shifting can be realized, which can be divided into several groups. Each group can be utilized to realize a specific function, such as an MPF, an OBFN, a phase-coded/LFM signal generator, and RF interference cancellations. Since the orthogonally polarized wavelength generator is shared by all the functions, the multi-functional signal processor would be compact, and the cost can be significantly reduced. The multi-functionality of the polarization-based photonic microwave phase shifter makes it more attractive for multi-functional and multi-band radar systems.

Although the polarization-based photonic microwave phase shifters are flexible in many applications, they are currently implemented by discrete components, making the system bulky and sensitive to the environmental vibrations, which would confine their applications (e.g., the onboard and satellite-board radars). A promising solution to this problem is using integrated microwave photonic technologies. Since most of the devices used in the polarization-based photonic microwave phase shifters can be implemented in an integrated photonics chip, e.g., lasers [102], [103], PDM-DPMZMs [44], polarizers [104]–[106], wavelength division multiplexer (WDM) [107], delay lines [108], and PDs [109], [110], polarization-based photonic microwave phase shifters have the potential to be integrated in a single chip in the future, which would significantly reduce the size of the system and make the system more suitable for practical applications.

Acknowledgements

The authors would like to thank Dr. Fangzhen Zhang, Dr. Dan Zhu, Dr. Yu Xiang, Mr. Zhaoyu Li, and Mr. JingzhanShi for their technical support and help.

References

[1] M. I. Skolnik, Ed., *Radar Handbook*, 2nd ed. New York, NY, USA: McGraw-Hill, 1991.
[2] S. Pan, D. Zhu, and F. Zhang, "Microwave photonics for modern radar systems," *Trans. Nanjing Univ. Aeronaut. Astronaut.*, vol. 31, no. 3, pp. 219–240, Jun. 2014.
[3] P. Ghelfi *et al.*, "A fully photonics-based coherent radar system," *Nature*, vol. 507, no. 7492, pp. 341–345, Mar. 2014.
[4] A. V. Oppenheim, *Discrete-Time Signal Processing*. Upper Saddle River, NJ, USA: Person Education, 1999.
[5] P. Allen and D. Holberg, *CMOS Analog Circuit Design*, 1st ed. London, U.K.: Oxford Univ. Press, 1987.
[6] R. Gregorian and G. Temes, *Analog MOS Integrated Circuits for Signal Processing*. New York, NY, USA: Wiley, 1986.
[7] J. Capmany and D. Novak, "Microwave photonics combines two worlds," *Nature Photon.*, vol. 1, no. 6, pp. 319–330, Jun. 2007.
[8] J. Yao, "Microwave photonics," *J. Lightw. Technol.*, vol. 27, no. 3, pp. 314–335, Feb. 1, 2009.
[9] R. A. Minasian, E. H. W. Chan, and X. Yi, "Microwave photonic signal processing," *Opt. Express*, vol. 21, no. 19, pp. 22918–22936, Sep. 2013.
[10] J. Capmany, J. Mora, I. Gasulla, J. Sancho, J. Lloret, and S. Sales, "Microwave photonic signal processing," *J. Lightw. Technol.*, vol. 31, no. 4, pp. 571–586, Feb. 15, 2013.
[11] M. Pagani, D. Marpaung, D.-Y. Choi, S. J. Madden, B. Luther-Davies, and B. J. Eggleton, "Tunable wideband microwave photonic phase shifter using on-chip stimulated Brillouin scattering," *Opt. Express*, vol. 22, no. 23, pp. 28810–28818, Nov. 2014.
[12] J. Sancho, J. Lloret, I. Gasulla, S. Sales, and J. Capmany, "Fully tunable 360° microwave photonic phase shifter based on a single semiconductor optical amplifier," *Opt. Express*, vol. 19, no. 18, pp. 17421–17426, Sep. 2011.
[13] W. Xue, S. Sales, J. Capmany, and J. Mørk, "Wideband 360° microwave photonic phase shifter based on slow light in semiconductor optical amplifiers," *Opt. Express*, vol. 18, no. 6, pp. 6156–6163, Mar. 2010.
[14] H. Shahoei and J. P. Yao, "Tunable microwave photonic phase shifter based on slow and fast light effects in a tilted fiber Bragg grating," *Opt. Express*, vol. 20, no. 13, pp. 14009–14014, Jun. 2012.
[15] M. Pu *et al.*, "Widely tunable microwave phase shifter based on silicon-on-insulator dual-microring resonator," *Opt. Express*, vol. 18, no. 6, pp. 6172–6182, Mar. 2010.
[16] P. Qu *et al.*, "Design of a vector-sum integrated microwave photonic phase shifter in silicon-on-insulator waveguides," *Appl. Opt.*, vol. 50, no. 17, pp. 2523–2530, Sep. 2011.
[17] L. A. Bui, A. Mitchell, K. Ghorbani, and T.-H. Chio, "Wide-band RF photonic second order vector sum phase-shifter," *IEEE Microw. Wireless Compon. Lett.*, vol. 15, no. 5, pp. 309–311, May 2005.
[18] X. Wang, T. Niu, E. H. W. Chan, X. Feng, B.-O. Guan, and J. Yao, "Photonics-based wideband microwave phase shifter," *IEEE Photon. J.*, vol. 9, no. 3, Jun. 2017, Art. no. 5501710.
[19] W. Li, W. Zhang, and J. Yao, "A wideband 360° photonic-assisted microwave phase shifter using a polarization modulator and a polarization-maintaining fiber Bragg grating," *Opt. Express*, vol. 20, no. 28, pp. 29838–29843, Dec. 2012.
[20] W. Li, W. H. Sun, W. T. Wang, L. X. Wang, J. G. Liu, and N. H. Zhu, "Photonic-assisted microwave phase shifter using a DMZM and an optical bandpass filter," *Opt. Express*, vol. 22, no. 5, pp. 5522–5527, Mar. 2014.
[21] E. H. W. Chan, W. Zhang, and R. A. Minasian, "Photonic RF phase shifter based on optical carrier and RF modulation sidebands amplitude and phase control," *J. Lightw. Technol.*, vol. 30, no. 23, pp. 3672–3678, Dec. 1, 2012.
[22] H. Y. Jiang *et al.*, "Microwave photonic phase shifter using a phase modulator and a fiber Bragg grating in a round-trip," in *Proc. IEEE Conf. Lasers Electro-Opt.*, Jun. 2013, pp. 1–2, Paper CTu3G.6.
[23] S. Pan and Y. Zhang, "Tunable and wideband microwave photonic phase shifter based on a single-sideband polarization modulator and a polarizer," *Opt. Lett.*, vol. 37, no. 21, pp. 4483–4485, Nov. 2012.
[24] H. Chen, Y. Dong, H. He, W. Hu, and L. Li, "Photonic radio-frequency phase shifter based on polarization interference," *Opt. Lett.*, vol. 34, no. 15, pp. 2375–2377, 2009.
[25] W. Li, F. Kong, and J. Yao, "Arbitrary microwave waveform generation based on a tunable optoelectronic oscillator," *J. Lightw. Technol.*, vol. 31, no. 23, pp. 3780–3786, Dec. 1, 2013.
[26] X. Li, S. Zhao, S. Pan, and Z. Zhu, "Generation of an orthogonally polarized dual-wavelength optical signal with large wavelength-spacing tunability by using an integrated modulator and a Sagnac loop," *Opt. Quant. Electron.*, vol. 49, no. 11, 2017, Art. no. 364.
[27] Z. Li *et al.*, "Linear photonic radio frequency phase shifter using a differential-group-delay element and an optical phase modulator," *Opt. Lett.*, vol. 35, no. 11, pp. 1881–1883, Jun. 2010.
[28] H. Chi and J. Yao, "Photonic generation of phase-coded millimeter-wave signal using a polarization modulator," *IEEE Microw. Wireless Compon. Lett.*, vol. 18, no. 5, pp. 371–373, May 2008.
[29] Z. Li, M. Li, H. Chi, X. Zhang, and J. Yao, "Photonic generation of phase-coded millimeter-wave signal with large frequency tunability using a polarization-maintaining fiber Bragg gratingg," *IEEE Microw. Wireless Compon. Lett.*, vol. 21, no. 12, pp. 694–696, Dec. 2011.
[30] M. Sagues and A. Loayssa, "Orthogonally polarized optical single sideband modulation for microwave photonics processing using stimulated Brillouin scattering," *Opt. Express*, vol. 18, no. 22, pp. 22906–22914, Oct. 2010.
[31] W. Li, N. H. Zhu, and L. X. Wang, "Perfectly orthogonal optical single-sideband signal generation based on stimulated Brillouin scattering," *IEEE Photon. Technol. Lett.*, vol. 24, no. 9, pp. 751–753, May 1, 2012.
[32] Y. Zhang, F. Zhang, and S. Pan, "Optical single sideband polarization modulation for radio-over-fiber system and microwave photonic signal processing," *Photon. Res.*, vol. 2, no. 4, pp. B80–B85, Aug. 2014.

[33] S. Liu, D. Zhu, Z. Wei, and S. Pan, “Photonic generation of widely tunable phase-coded microwave signals based on a dual-parallel polarization modulator,” *Opt. Lett.*, vol. 39, no. 13, pp. 3958–3961, Jul. 2014.

[34] W. Zhang and J. Yao, “Ultrawideband RF photonic phase shifter using two cascaded polarization modulators,” *IEEE Photon. Technol. Lett.*, vol. 26, no. 9, pp. 911–914, May 1, 2014.

[35] Y. Zhang, F. Zhang, and S. Pan, “Frequency-doubled and phase-coded RF signal generation based on orthogonally polarized carrier-suppressed double sideband modulation,” in *Proc. Asia Commun. Photon. Conf. (ACP)*, Shanghai, China, Nov. 2014, pp. 11–14, Paper AF3A.2.

[36] Y. Zhang, F. Zhang, and S. Pan, “Generation of frequency-multiplied and phase-coded signal using an optical polarization division multiplexing modulator,” *IEEE Trans. Microw. Theory Techn.*, vol. 65, no. 2, pp. 651–660, Feb. 2017.

[37] Y. Zhang and S. Pan, “Frequency-multiplying microwave photonic phase shifter for independent multichannel phase shifting,” *Opt. Lett.*, vol. 41, no. 6, pp. 1261–1264, Mar. 2016.

[38] Y. Zhang and S. Pan, “Photonics-based multi-function analog signal processor based on a polarization division multiplexing Mach–Zehnder modulator,” *Opt. Lett.*, vol. 42, no. 23, pp. 5034–5037, Dec. 2017.

[39] L. Thevenaz, A. Zadok, A. Eyal, and M. Tur, “All-optical polarization control through Brillouin amplification,” in *Proc. Opt. Fiber Commun. Conf. (OFC)*, 2008, pp. 1–3, Paper OML7.

[40] H. Soto, D. Erasme, and G. Guekos, “Cross-polarization modulation in semiconductor optical amplifier,” *IEEE Photon. Technol. Lett.*, vol. 11, no. 8, pp. 970–972, Aug. 1999.

[41] J. Y. Lee, L. Yin, G. P. Agrawal, and P. M. Fauchet, “Ultrafast optical switching based on nonlinear polarization rotation in silicon waveguides,” *Opt. Express*, vol. 18, no. 11, pp. 11514–11523, May 2010.

[42] E. Compain and B. Drevillon, “High-frequency modulation of the four states of polarization of light with a single phase modulator,” *Rev. Sci. Instrum.*, vol. 69, no. 4, pp. 1574–1580, Apr. 1998.

[43] J. D. Bull, N. A. F. Jaeger, H. Kato, M. Fairburn, A. Reid, and P. Ghanipour, “40-GHz electro-optic polarization modulator for fiber optic communications systems,” *Proc. SPIE*, vol. 5577, pp. 133–144, Dec. 2004.

[44] P. Dong, C. Xie, L. Chen, L. L. Buhl, and Y.-K. Chen, “112-Gb/s monolithic PDM-QPSK modulator in silicon,” *Opt. Express*, vol. 20, no. 26, p. B624-629, Dec. 2012.

[45] S. Pan, P. Zhou, Z. Tang, F. Zhang, and D. Zhu, “Optoelectronic oscillator based on polarization modulation,” *Fiber Integr. Opt.*, vol. 34, no. 4, pp. 185–203, Oct. 2015.

[46] J. Yao, “Photonics to the rescue: A fresh look at microwave photonic filters,” *IEEE Microw. Mag.*, vol. 16, no. 8, pp. 46–60, Sep. 2015.

[47] J. Capmany, B. Ortega, and D. Pastor, “A tutorial on microwave photonic filters,” *J. Lightw. Technol.*, vol. 24, no. 1, pp. 201–229, Jan. 2006.

[48] Z. Zhu, H. Chi, T. Jin, S. Zheng, X. Jin, and X. Zhang, “All-positive-coefficient microwave photonic filter with rectangular response,” *Opt. Lett.*, vol. 42, no. 15, pp. 3012–3015, Aug. 2017.

[49] J. Capmany, J. Mora, D. Pastor, and B. Ortega, “High-quality Online-reconfigurable microwave photonic transversal filter with positive and negative coefficients,” *IEEE Photon. Technol. Lett.*, vol. 17, no. 12, pp. 2730–2732, Dec. 2005.

[50] J. Capmany, D. Pastor, A. Martinez, B. Ortega, and S. Sales, “Microwave photonic filters with negative coefficients based on phase inversion in an electro-optic modulator,” *Opt. Lett.*, vol. 28, no. 16, pp. 1415–1417, Aug. 2013.

[51] F. Zeng, J. Wang, and J. Yao, “All-optical microwave bandpass filter with negative coefficients based on a phase modulator and linearly chirped fiber Bragg gratings,” *Opt. Lett.*, vol. 30, no. 17, pp. 2203–2205, Sep. 2005.

[52] J. Yao and Q. Wang, “Photonic microwave bandpass filter with negative coefficients using a polarization modulator,” *IEEE Photon. Technol. Lett.*, vol. 19, no. 9, pp. 644–646, May 1, 2007.

[53] M. Sagues, A. Loayssa, and J. Capmany, “Multitap complex-coefficient incoherent microwave photonic filters based on stimulated Brillouin scattering,” *IEEE Photon. Technol. Lett.*, vol. 19, no. 16, pp. 1194–1196, Aug. 15, 2007.

[54] W. T. Wang, J. G. Liu, H. K. Mei, W. Y. Wang, and N. H. Zhu, “Microwave photonic filter with complex coefficient based on optical carrier phase shift utilizing two stimulated Brillouin scattering pumps,” *IEEE Photon. J.*, vol. 7, no. 1, Feb. 2015, Art. no. 5500208.

[55] W. Xue, S. Sales, J. Mork, and J. Capmany, “Widely tunable microwave photonic notch filter based on slow and fast light effects,” *IEEE Photon. Technol. Lett.*, vol. 21, no. 3, pp. 167–169, Feb. 1, 2009.

[56] H. Shahoei and J. P. Yao, “A continuously tunable multi-tap complex-coefficient microwave photonic filter based on a tilted fiber Bragg grating,” *Opt. Express*, vol. 21, no. 6, pp. 7521–7527, Mar. 2013.

[57] V. R. Supradeepa *et al.*, “Comb-based radiofrequency photonic filters with rapid tunability and high selectivity,” *Nature Photon.*, vol. 6, pp. 186–194, Feb. 2012.

[58] W. Li, W. T. Wang, W. H. Sun, J. G. Liu, and N. H. Zhu, “Microwave photonic notch filter with complex coefficient based on DDMZM,” *IEEE Photon. Technol. Lett.*, vol. 26, no. 18, pp. 1859–1862, Sep. 15, 2014.

[59] Y. Zhang and S. Pan, “Complex coefficient microwave photonic filter using a polarization-modulator-based phase shifter,” *IEEE Photon. Technol. Lett.*, vol. 25, no. 2, pp. 187–189, Jan. 15, 2013.

[60] X. Li, J. Dong, Y. Yu, and X. Zhang, “A tunable microwave photonic filter based on an all-optical differentiator,” *IEEE Photon. Technol. Lett.*, vol. 23, no. 5, pp. 308–310, Mar. 1, 2011.

[61] Y. M. Zhang and S. L. Pan, “A tunable and dispersion-insensitive microwave photonic filter,” *Sci. China Technol. Sci.*, vol. 56, no. 3, pp. 603–607, Mar. 2013.

[62] X. Yi, T. X. H. Huang, and R. A. Minasian, “Tunable and reconfigurable photonic signal processor with programmable all-optical complex coefficients,” *IEEE Trans. Microw. Theory Techn.*, vol. 58, no. 11, pp. 3088–3093, Nov. 2010.

[63] Y. Zhang and S. Pan, “Tunable multitap microwave photonic filter with all complex coefficients,” *Opt. Lett.*, vol. 38, no. 5, pp. 802–804, Mar. 2013.

[64] A. Mokhtari, S. Preußler, K. Jamshidi, M. Akbari, and T. Schneider, “Fully-tunable microwave photonic filter with complex coefficients using tunable delay lines based on frequency-time conversions,” *Opt. Express*, vol. 20, no. 20, pp. 22728–22734, Oct. 2012.

[65] Z. Tang and S. Pan, “Image-reject mixer with large suppression of mixing spurs based on a photonic microwave phase shifter,” *J. Lightw. Technol.*, vol. 34, no. 20, pp. 4727–4735, Oct. 15, 2016.

[66] T. Jiang, R. Wu, S. Yu, D. Wang, and W. Gu, “Microwave photonic phase-tunable mixer,” *Opt. Express*, vol. 25, no. 4, pp. 4519–4527, Feb. 2017.

[67] X. Ye, F. Zhang, and S. Pan, “Compact optical true time delay beamformer for a 2D phased array antenna using tunable dispersive elements,” *Opt. Lett.*, vol. 41, no. 17, pp. 3956–3959, Aug. 2016.

[68] X. Ye, D. Zhu, Y. Zhang, S. Li, and S. Pan, “Analysis of photonics-based RF beamforming with large instantaneous bandwidth,” *J. Lightw. Technol.*, vol. 35, no. 23, pp. 5010–5019, Dec. 1, 2017.

[69] A. Meijerink *et al.*, “Novel ring resonator-based integrated photonic beamformer for broadband phased array receive antennas—Part I: Design and performance analysis,” *J. Lightw. Technol.*, vol. 28, no. 1, pp. 3–18, Jan. 1, 2010.

[70] N. A. Riza, “Analog vector modulation-based widely tunable frequency photonic beamformer for phased-array antennas,” *IEEE Trans. Microw. Theory Techn.*, vol. 45, no. 8, pp. 1508–1512, Aug. 1997.

[71] L. A. Bui, A. Mitchell, K. Ghorbani, T.-H. Chio, S. Mansoori, and E. R. Lopez, “Wide-band photonically phased array antenna using vector sum phase shifting approach,” *IEEE Trans. Antennas Propag.*, vol. 53, no. 11, pp. 3589–3596, Nov. 2005.

[72] X. Yi, T. X. H. Huang, and R. A. Minasian, “Photonic beamforming based on programmable phase shifters with amplitude and phase control,” *IEEE Photon. Technol. Lett.*, vol. 23, no. 18, pp. 1286–1288, Sep. 15, 2011.

[73] Y. M. Zhang, H. Wu, D. Zhu, and S. Pan, “An optically controlled phased array antenna based on single sideband polarization modulation,” *Opt. Express*, vol. 22, no. 4, pp. 3761–3765, Feb. 2014.

[74] A. Rashidinejad and A. M. Weiner, “Photonic radio-frequency arbitrary waveform generation with maximal time-bandwidth product capability,” *J. Lightw. Technol.*, vol. 32, no. 20, pp. 3383–3393, Oct. 15, 2014.

[75] L. Gao, X. Chen, and J. Yao, “Photonic generation of a phase-coded microwave waveform with ultrawide frequency tunable range,” *IEEE Photon. Technol. Lett.*, vol. 25, no. 10, pp. 899–902, May 15, 2013.

[76] W. Li, W. T. Wang, W. H. Sun, L. X. Wang, and N. H. Zhu, “Photonic generation of arbitrarily phase-modulated microwave signals based on a single DDMZM,” *Opt. Express*, vol. 22, no. 7, pp. 7446–7457, Apr. 2014.

[77] H.-Y. Jiang, L.-S. Yan, J. Ye, W. Pan, B. Luo, and X. Zou, “Photonic generation of phase-coded microwave signals with tunable carrier frequency,” *Opt. Lett.*, vol. 38, no. 8, pp. 1361–1363, Apr. 2013.

[78] P. Ghelfi, F. Scotti, F. Laghezza, and A. Bogoni, "Photonic generation of phase-modulated RF signals for pulse compression techniques in coherent radars," *J. Lightw. Technol.*, vol. 30, no. 11, pp. 1638–1644, Jun. 1, 2012.

[79] Z. Li, M. Li, H. Chi, X. Zhang, and J. Yao, "Photonic generation of phase-coded millimeter-wave signal with large frequency tunability using a polarization-maintaining fiber Bragg grating," *IEEE Microw. Wireless Compon. Lett.*, vol. 21, no. 12, pp. 694–696, Dec. 2011.

[80] Y. Zhang and S. Pan, "Generation of phase-coded microwave signals using a polarization-modulator-based photonic microwave phase shifter," *Opt. Lett.*, vol. 38, no. 5, pp. 766–768, Mar. 2013.

[81] W. Li and J. Yao, "Generation of linearly chirped microwave waveform with an increased time-bandwidth product based on a tunable optoelectronic oscillator and a recirculating phase modulation loop," *J. Lightw. Technol.*, vol. 32, no. 20, pp. 3573–3579, Oct. 15, 2014.

[82] Y. Zhang, X. Ye, Q. Guo, F. Zhang, and S. Pan, "Photonic generation of linear-frequency-modulated waveforms with improved time-bandwidth product based on polarization modulation," *J. Lightw. Technol.*, vol. 35, no. 10, pp. 1821–1829, May 15, 2017.

[83] A. K. Poddar, U. L. Rohde, and A. M. Apte, "How low can they go?: Oscillator phase noise model, theoretical, experimental validation, and phase noise measurements," *IEEE Microw. Mag.*, vol. 14, no. 6, pp. 50–72, Sep./Oct. 2013.

[84] E. Rubiola, E. Salik, S. Huang, N. Yu, and L. Maleki, "Photonic-delay technique for phase-noise measurement of microwave oscillators," *J. Opt. Soc. Amer. B, Opt. Phys.*, vol. 22, no. 5, pp. 987–997, May 2005.

[85] U. L. Rohde, A. K. Poddar, and A. M. Apte, "Getting its measure: Oscillator phase noise measurement techniques and limitations," *IEEE Microw. Mag.*, vol. 14, no. 16, pp. 73–86, Sep./Oct. 2013.

[86] A. Lance, W. D. Seal, and F. Labaar, "Phase noise and AM noise measurements in the frequency domain," *Infr. Millim. Waves*, vol. 11, pp. 239–289, Oct. 1984.

[87] K. Volyanskiy *et al.*, "Applications of the optical fiber to the generation and measurement of low-phase-noise microwave signals," *J. Opt. Soc. Amer. B, Opt. Phys.*, vol. 25, no. 12, pp. 2140–2150, Dec. 2008.

[88] X. S. Yao and L. Maleki, "Multiloop optoelectronic oscillator," *IEEE J. Quantum Electron.*, vol. 36, no. 1, pp. 79–84, Jan. 2000.

[89] J. Hong, A.-M. Liu, and J. Guo, "Study on low-phase-noise optoelectronic oscillator and high-sensitivity phase noise measurement system," *J. Opt. Soc. Amer. A, Opt. Image Sci.*, vol. 30, no. 8, pp. 1557–1562, Aug. 2013.

[90] D. Zhu, F. Zhang, P. Zhou, and S. Pan, "Phase noise measurement of wideband microwave sources based on a microwave photonic frequency down-converter," *Opt. Lett.*, vol. 40, no. 7, pp. 1326–1329, Apr. 2015.

[91] D. Zhu, F. Zhang, P. Zhou, D. Zhu, and S. Pan, "Wideband phase noise measurement using a multifunctional microwave photonic processor," *IEEE Photon. Technol. Lett.*, vol. 26, no. 24, pp. 2434–2437, Dec. 15, 2014.

[92] N. Kuse and M. E. Fermann, "Electro-optic comb based real time ultra-high sensitivity phase noise measurement system for high frequency microwaves," *Sci. Rep.*, vol. 7, p. 2847, Jun. 2017.

[93] E. J. Adles, T. R. Clark, M. L. Dennis, A. M. Karim, and T. P. McKenna, "Interferer cancellation in coherent optical RF receivers via optical phase modulation," in *Proc. IEEE Photon. Conf.*, Sep. 2012, pp. 218–219.

[94] V. J. Urick, J. F. Diehl, C. E. Sunderman, J. D. McKinney, and K. J. Williams, "An optical technique for radio frequency interference mitigation," *IEEE Photon. Technol. Lett.*, vol. 27, no. 12, pp. 1333–1336, Jun. 15, 2015.

[95] M. P. Chang, M. Fok, A. Hofmaier, and P. R. Prucnal, "Optical analog self-interference cancellation using electro-absorption modulators," *IEEE Microw. Wireless Compon. Lett.*, vol. 23, no. 2, pp. 99–101, Feb. 2013.

[96] M. Huang, D. Zhu, and S. Pan, "Optical RF interference cancellation based on a dual-parallel polarization modulator," in *Proc. Asia Commun. Photon. Conf.*, 2014, Paper ATh1F.6. [Online]. Available: https://www.osapublishing.org/abstract.cfm?uri=ACPC-2014-ATh1F.6

[97] J. Suarez and P. R. Prucnal, "Instantaneous bandwidth of counter-phase optical interference cancellation for RF communications," *IEEE Microw. Wireless Compon. Lett.*, vol. 21, no. 9, pp. 507–509, Sep. 2011.

[98] W. Zhou, P. Xiang, Z. Niu, M. Wang, and S. Pan, "Wideband optical multipath interference cancellation based on a dispersive element," *IEEE Photon. Technol. Lett.*, vol. 28, no. 8, pp. 849–851, Apr. 15, 2016.

[99] G. Li, Y. Xiang, and S. Pan, "Wideband optical cancellation of RF interference with phase change," in *Proc. Int. Conf. Opt. Commun. Netw. (ICOCN)*, Wuzheng, China, Aug. 2017, pp. 1–3.

[100] Y. Xiang, G. Li, and S. Pan, "Ultrawideband optical cancellation of RF interference with phase change," *Opt. Express*, vol. 25, no. 18, pp. 21259–21264, Sep. 2017.

[101] Z. Li, Y. Han, H. Chi, X. Zhang, and J. Yao, "A continuously tunable microwave fractional Hilbert transformer based on a nonuniformly spaced photonic microwave delay-line filter," *J. Lightw. Technol.*, vol. 30, no. 12, pp. 1948–1953, Jun. 2012.

[102] P. Del'Haye, A. Schliesser, O. Arcizet, T. Wilken, R. Holzwarth, and T. J. Kippenberg, "Optical frequency comb generation from a monolithic microresonator," *Nature*, vol. 450, no. 7173, pp. 1214–1217, Dec. 2007.

[103] H. Rong *et al.*, "A continuous-wave Raman silicon laser," *Nature*, vol. 433, no. 7027, pp. 725–728, Feb. 2005.

[104] W. D. Sacher, T. Barwicz, B. J. F. Taylor, and J. K. S. Poon, "Polarization rotator-splitters in standard active silicon photonics platforms," *Opt. Express*, vol. 22, no. 4, pp. 3777–3786, 2014.

[105] I. Kiyat, A. Aydinli, and N. Dagli, "A compact silicon-on-insulator polarization splitter," *IEEE Photon. Technol. Lett.*, vol. 17, no. 1, pp. 100–102, Jan. 2005.

[106] T. K. Liang and H. K. Tsang, "Integrated polarization beam splitter in high index contrast silicon-on-insulator waveguides," *IEEE Photon. Technol. Lett.*, vol. 17, no. 2, pp. 393–395, Feb. 2005.

[107] D. T. H. Tan *et al.*, "Wide bandwidth, low loss 1 by 4 wavelength division multiplexer on silicon for optical interconnects," *Opt. Express*, vol. 19, no. 3, pp. 2401–2409, Jan. 2011.

[108] Y. Liu, A. Choudhary, D. Marpaung, and B. J. Eggleton, "Gigahertz optical tuning of an on-chip radio frequency photonic delay line," *Optica*, vol. 4, no. 4, pp. 418–423, 2017.

[109] X. Yi, S. X. Chew, S. Song, L. Nguyen, and R. Minasian, "Integrated microwave photonics for wideband signal processing," *Photonics*, vol. 4, no. 4, p. 46, Nov. 2017.

[110] D. Marpaung, C. Roeloffzen, R. Heideman, A. Leinse, S. Sales, and J. Capmany, "Integrated microwave photonics," *Lasers Photon. Rev.*, vol. 7, no. 4, pp. 506–538, Jul. 2013.

Yamei Zhang (S'13) received the B.S. degree from the Nanjing University of Aeronautics and Astronautics, Nanjing, China, in 2012, where she is currently pursuing the Ph.D. degree with the Key Laboratory of Radar Imaging and Microwave Photonics, Ministry of Education.

Her current research focuses on microwave photonic signal generation and processing.

Shilong Pan (S'06–M'09–SM'13) received the B.S. and Ph.D. degrees in electronics engineering from Tsinghua University, Beijing, China, in 2004 and 2008, respectively.

From 2008 to 2010, he was a Vision 2010 Post-Doctoral Research Fellow with the Microwave Photonics Research Laboratory, University of Ottawa, Canada. He joined the College of Electronic and Information Engineering, Nanjing University of Aeronautics and Astronautics, China, in 2010, where he is currently a Full Professor and an Executive Director of the Key Laboratory of Radar Imaging and Microwave Photonics, Ministry of Education.

He has authored or co-authored over 360 research papers, including over 190 papers in peer-reviewed journals and 170 papers in conference proceedings. His research has focused on microwave photonics, which includes optical generation and processing of microwave signals, analog photonic links, photonic microwave measurement, and integrated microwave photonics.

Dr. Pan is currently a Topical Editor of *Chinese Optics Letters*. He was selected to receive the OSA Outstanding Reviewer Award in 2015. He was a Top Reviewer for the *Journal of Lightwave Technology* in 2016. He serves as the chair of numerous international conferences and workshops, including the TPC Chair of the International Conference on Optical Communications and Networks in 2015, the TPC Co-Chair of the IEEE International Topical Meeting on Microwave Photonics in 2017, the TPC Chair of the high-speed and broadband wireless technologies subcommittee of the IEEE Radio Wireless Symposium in 2013, 2014, and 2016, the TPC Chair of the optical fiber sensors and microwave photonics subcommittee of the OptoElectronics and Communication Conference in 2015, and the Chair of the microwave photonics for broadband measurement workshop of the International Microwave Symposium in 2015.